



The quorum-quenching lactonase from *Alicyclobacter acidoterrestris*: purification, kinetic characterization, crystallization and crystallographic analysis

Celine Bergonzi, Michael Schwab, Eric Chabriere and Mikael Elias

Acta Cryst. (2017). **F73**, 476–480



IUCr Journals
CRYSTALLOGRAPHY JOURNALS ONLINE

Copyright © International Union of Crystallography

Author(s) of this paper may load this reprint on their own web site or institutional repository provided that this cover page is retained. Republication of this article or its storage in electronic databases other than as specified above is not permitted without prior permission in writing from the IUCr.

For further information see <http://journals.iucr.org/services/authorrights.html>

The quorum-quenching lactonase from *Alicyclobacter acidoterrestris*: purification, kinetic characterization, crystallization and crystallographic analysis

Celine Bergonzi,^{a,b} Michael Schwab,^a Eric Chabriere^b and Mikael Elias^{a*}

Received 2 June 2017

Accepted 18 July 2017

Edited by L. J. Beamer, University of Missouri, USA

Keywords: quorum sensing; quorum quenching; lactonases; thermophiles; *Alicyclobacter acidoterrestris*.

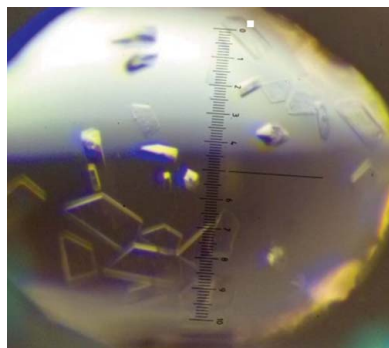
^aBiochemistry, Molecular Biology and Biophysics Department and BioTechnology Institute, University of Minnesota, Saint Paul, MN 55108, USA, and ^bURMITE, Aix Marseille Université, INSERM, CNRS, IRD, 27 Boulevard Jean Moulin, 13385 Marseille, France. *Correspondence e-mail: mhelias@umn.edu

Lactonases comprise a class of enzymes that hydrolyze lactones, including acyl-homoserine lactones (AHLs); the latter are used as chemical signaling molecules by numerous Gram-negative bacteria. Lactonases have therefore been demonstrated to quench AHL-based bacterial communication. In particular, lactonases are capable of inhibiting bacterial behaviors that depend on these chemicals, such as the formation of biofilms or the expression of virulence factors. A novel representative from the metallo- β -lactamase superfamily, named AaL, was isolated from the thermoacidophilic bacterium *Alicyclobacter acidoterrestris*. Kinetic characterization proves AaL to be a proficient lactonase, with catalytic efficiencies (k_{cat}/K_m) against AHLs in the region of $10^5 \text{ M}^{-1} \text{ s}^{-1}$. AaL exhibits a very broad substrate specificity. Its structure is expected to reveal the molecular determinants for its substrate binding and specificity, as well as to provide grounds for future protein-engineering projects. Here, the expression, purification, characterization, crystallization and X-ray diffraction data collection of AaL at 1.65 Å resolution are reported.

1. Introduction

Quorum sensing (QS) is a chemical communication mechanism used by microbes to coordinate behavior in a cell-density-dependent manner, such as in bioluminescence, biofilm formation, expression of virulence factors, swarming motility and many others (Bassler, 1999; Miller & Bassler, 2001). QS utilizes a variety of small diffusible molecules, including acyl-homoserine lactones (AHLs). AHLs can significantly vary with regard to their alkyl chain, which typically ranges from four to 14 C atoms and may include various chemical modifications [for example oxidation on carbon 3 (Lade *et al.*, 2014) or a *p*-coumaroyl substituent (Schaefer *et al.*, 2008)]. Quorum sensing can be quenched by enzymes called lactonases, which can catalyze the opening of the lactone ring (Bokhove *et al.*, 2010; Hiblot, Gotthard, Elias *et al.*, 2013).

AHL-degrading enzymes can be found in organisms beyond the bacterial world, and have been isolated from archaea, plants, fungi and mammals in addition to bacteria (LaSarre & Federle, 2013; Elias & Tawfik, 2012). Three large families of lactonases have been identified (Elias & Tawfik, 2012), and the three families have distinct structural properties. The paraxonases, which exhibit a six-bladed β -propeller fold (Ben-David *et al.*, 2013, 2015), have been shown to proficiently hydrolyze δ -lactones, γ -lactones and AHLs (Bar-Rogovsky *et al.*, 2013; Khersonsky & Tawfik, 2005). Another family, the phosphotriesterase-like lactonases (PLLs), which exhibit a



© 2017 International Union of Crystallography

Table 1
Expression and production of AaL.

Source organism	<i>A. acidoterrestris</i>
DNA source	Synthetic
Cloning vector	pET-22b(+)
Expression vector	pET-22b(+)
Expression host	<i>E. coli</i>
Restriction sites	NdeI, XhoI
Complete amino-acid sequence of the construct produced	SMTNIAKAQPKLYVMDNGRMRMDKNWMIAMHNPA-TIANPNAPTEFIEFPYITVLIDHPEGKILFDT-SCNPDSMGAQGRWGEATQSMFPWTASEECYLH-NRLEQLKVRPEDIKFVIAASHLHLDHAGCLEMF-TNATIIVHEDEFSGALQTYARNQTEGAYIWGD-IDAWIKNNLNWRTIKRDEDNIVLAEGIKILNF-GSGHAWGMLGLHVQLPEKGGIILASDAVYSAE-SYGPPIKPPGIIYDSLGFVRSVEKIKRIAKET-NSEVWFGHDSEQFKRFRKSTEGYYETAGTAG

(β/α)₈ fold, have been identified from numerous bacterial and archaeal sources, including extremophiles (Xiang *et al.*, 2009; Hawwa *et al.*, 2009; Afriat *et al.*, 2006; Elias *et al.*, 2008; Del Vecchio *et al.*, 2009; Hiblot *et al.*, 2012, 2015; Bzdrenga *et al.*, 2014; Hiblot, Gotthard, Elias *et al.*, 2013). PLLs show different substrate specificities and were divided accordingly: PLL-As can hydrolyze δ -lactones, γ -lactones and AHLs, whereas PLL-Bs prefer δ -lactones and γ -lactones (Hiblot *et al.*, 2015).

The third family of lactonases are the metallo- β -lactamase-like lactonases (MLLs), illustrated by the first isolated and most studied representative: autoinducer inactivator A (AiiA) from *Bacillus thuringiensis*. The crystal structure of AiiA has been determined (Liu *et al.*, 2005) and its catalytic mechanism has been investigated (Liu *et al.*, 2008; Momb *et al.*, 2008). Owing to its ability to disrupt bacterial quorum sensing, AiiA has been shown to protect plants from bacterial infection in a genetically modified plant system (Dong *et al.*, 2000) as well as inhibiting bacterial biofilm formation (Augustine *et al.*, 2010).

AaL (WP_021296945.1) is a recently identified enzyme that was isolated from the acidophilic, moderately thermostable bacterium *Alicyclobacter acidoterrestris*. *A. acidoterrestris* exhibits a broad growth-temperature range (25–60°C) and can grow at various pH values (pH 2.5–6.0) (Spinelli *et al.*, 2009). AaL is a rare representative of the MLL family in thermophilic organisms: it shares 27% sequence identity with AiiA and 43% sequence identity with the closest known structure, AiiB (PDB entry 2r2d; Liu *et al.*, 2007). AaL also shares 85% sequence identity with the recently crystallized lactonase GcL from *Geobacillus caldoxylosilyticus* (Bergonzi *et al.*, 2016). Here, we report the protein production, purification, kinetic characterization, crystallization and preliminary X-ray diffraction data of the lactonase AaL.

2. Materials and methods

2.1. Cloning, expression and purification of AaL

The gene encoding AaL in the organism *A. acidoterrestris* (WP_021296945.1) was optimized for heterologous expression in *Escherichia coli* and was synthesized by GenScript (Piscataway, New Jersey, USA) (Table 1). The gene construct includes an N-terminal affinity Strep-tag (WSHPQFEK)

followed by a TEV cleavage site (ENLYFQS) to allow nearly complete removal of the tag, leaving only an N-terminal serine residue after cleavage. The optimized AaL gene construct was cloned in pET-22b(+) (Novagen) using NdeI and XhoI as restriction sites.

The protein was overproduced as described previously (Hiblot, Gotthard, Champion *et al.*, 2013; Hiblot *et al.*, 2012, 2015; Gotthard *et al.*, 2011; Bergonzi *et al.*, 2016). Protein expression was carried out in 1 l ZYP autoinducer medium (100 $\mu\text{g ml}^{-1}$ ampicillin and 34 $\mu\text{g ml}^{-1}$ chloramphenicol), inoculated with 10 ml of overnight pre-culture. Cell cultures were grown at 309 K until they reached the exponential growth phase (OD_{600 nm}). The cell cultures then underwent a temperature transition at 290 K overnight, and 0.2 mM CoCl₂ was added to the medium to assist proper folding of the metalloenzyme. The induction of AaL is caused by a shortage of glucose and the import of lactose from the autoinducer medium. The cells were pelleted by centrifugation at 272 K (4400g, 15 min). The pellets were resuspended in a lysis buffer composed of 50 mM HEPES pH 8, 150 mM NaCl, 0.2 mM CoCl₂, 0.25 mg ml⁻¹ lysozyme, 0.1 mM phenylmethylsulfonyl fluoride (PMSF). Cell lysis was performed using a sonication device (Q700 Sonicator, Qsonica, USA) through three sonication steps of 30 s at an amplitude of 45 (1 s pulse on; 1 s pulse off). Cell debris was removed by centrifugation at 272 K (5000g, 20 min) and the lysate was filtered using 0.22 μm filters (VWR, USA). The filtered lysate was subsequently applied onto a StrepTrap HP column (GE Healthcare) using a flow rate of 1 ml min⁻¹. AaL was eluted with an elution buffer consisting of 50 mM HEPES pH 8, 150 mM NaCl, 2.5 mM desthiobiotin. Pure fractions were pooled and cleaved with TEV protease overnight at room temperature. The protein

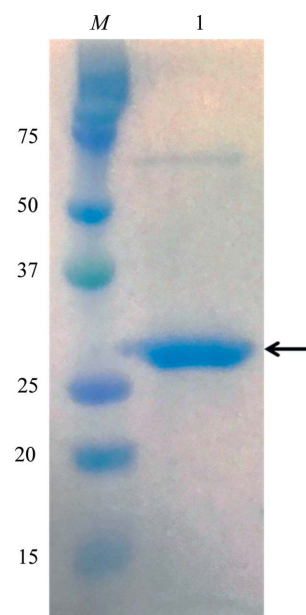


Figure 1
12% SDS-PAGE of the AaL protein. Lane M contains molecular-weight markers (Precision Plus Protein Kaleidoscope Prestained Protein Standards from Bio-Rad; labelled in kDa). Lane 1 contains 10 μl AaL protein at 2.5 mg ml⁻¹. The black arrow indicates the band for AaL.

Table 2
Kinetic parameters of AaL at 25°C.

	k_{cat} (s ⁻¹)	K_m (μM)	k_{cat}/K_m (s ⁻¹ M ⁻¹)
C4-AHL	13.54 ± 0.91	10.5 ± 0.3	(1.29 ± 0.37) × 10 ⁶
C6-AHL	13.97 ± 0.43	82.7 ± 11.0	(1.69 ± 0.23) × 10 ⁵
C10-AHL	5.13 ± 0.35	49.6 ± 1.4	(1.03 ± 0.30) × 10 ⁵
3-Oxo-C12-AHL	5.03 ± 0.25	14.0 ± 3.4	(3.60 ± 0.88) × 10 ⁵

sample was filtered to remove the precipitated TEV protease (0.22 μm filters; VWR, USA) and loaded onto a size-exclusion column (HiLoad 16/600, Superdex 200, GE Healthcare) equilibrated in a buffer composed of 50 mM HEPES pH 8.00, 150 mM NaCl. Fractions containing nearly pure AaL protein were pooled and concentrated to 10 mg ml⁻¹ using a centrifugation device (Vivaspin 15R, Sartorius, Germany). The yield was approximately 10 mg of nearly pure protein per litre of culture. The purity of the produced protein was assessed by Coomassie-stained SDS-PAGE (Fig. 1), revealing a band at ~32.5 kDa that corresponds to monomeric AaL.

2.2. Kinetic characterization of AaL

Kinetic measurements were performed in triplicate at 298 K on a microplate spectrophotometer (Synergy HTX, BioTek, USA) running the *Gen5.1* software (Table 2). In these experiments, a 200 μl reaction volume was used in a 96-well plate setup. Catalytic parameters were calculated by fitting the measured kinetic data to the Michaelis–Menten equation using the *GraphPad Prism 5.0* software. The time course of lactone hydrolysis was monitored by a previously described pH-indicator assay using cresol purple (Bergonzi *et al.*, 2016). Lactone hydrolysis generates a proton that subsequently acidifies the medium. The reaction rates can therefore be monitored at 577 nm in a weak buffer solution composed of 2.5 mM Bicine pH 8.3, 150 mM NaCl, 0.2 mM cresol purple and 0.5% DMSO over a range of substrate concentrations (0–2 mM). The extinction coefficient of cresol purple at pH 8.3 ($\epsilon_{577 \text{ nm}} = 2923 \text{ M}^{-1} \text{ cm}^{-1}$) was evaluated *in situ* by measuring the absorbance of the buffer with different concentrations of acetic acid (0–0.35 mM). A background rate was observed in the absence of substrate and enzyme, presumably corresponding to acidification by atmospheric CO₂. This rate (–4 to –8 mOD min⁻¹), which was independent of the substrate concentration, was subtracted from all measurements as described previously (Khersonsky & Tawfik, 2005). This rate was <5% of the rate observed with the enzyme.

2.3. Thermal stability of AaL

The thermal stability of the enzyme against heat was determined using the ANS (8-anilino-1-naphthalene-sulfonic acid) fluorescence thermal shift assay (Fig. 2; Hawe *et al.*, 2008). Triplicate samples (250 μl) containing 2.5 μM pure enzyme and 10 μM ANS were prepared. The samples were vortexed and incubated for 30 min at 25, 37, 45, 50, 55, 60, 70 and 80°C in different heating blocks. The samples were then assayed in a black, 96-well flat-bottom plate (Flat bottom 96 well, Fisherbrand) and measured using a fluorescence

Table 3
Crystallization of AaL.

Method	Sitting-drop vapor diffusion
Plate type	24-well plate
Temperature (K)	292
Protein concentration (mg ml ⁻¹)	10
Buffer composition of protein solution	50 mM HEPES pH 8.00, 150 mM NaCl
Composition of reservoir solution	0.45 M ammonium chloride, 16% polyethylene glycol 3350
Volume and ratio of drop	1:1
Volume of reservoir (μl)	500

microplate reader (Synergy HTX, BioTek, USA) with the *Gen5.1* software, using an excitation wavelength of 360 nm and an emission wavelength of 508 nm. The melting temperature of the enzyme (T_m), defined here as the temperature at which 50% of the maximal ANS fluorescence was reached, was determined by fitting the ANS fluorescence signal to the following equation at different tested temperatures using the *GraphPad Prism* software,

$$Y = \text{Bottom} + \frac{(\text{Top} - \text{Bottom})}{1 + \exp\left(\frac{T_m - X}{h}\right)}, \quad (1)$$

where X , Y and h represent the incubation temperature, the ANS fluorescence and the slope coefficient, respectively.

2.4. Crystallization of AaL

Purified and concentrated AaL samples (10 mg ml⁻¹) were subjected to crystallization trials (Table 3) using the sitting-drop vapor-diffusion method in a 96-well plate with the commercial kit JCSG+. Different protein:precipitant ratios were tested (1:1, 1:2 and 1:3) and the plate was incubated at 292 K. Small crystals appeared after 1 d at 292 K in a condition consisting of 0.45 M ammonium chloride, 16% polyethylene glycol 3350. In order to improve the crystal shape and size, micro-seeding was performed. A drop containing small protein crystals was pipetted, diluted, placed in 10 μl mother solution and vortexed for 30 s. This seed solution was diluted 75-fold and 0.1 μl of this diluted seeding solution was added to drops formed of 1 μl protein solution and 1 μl precipitant

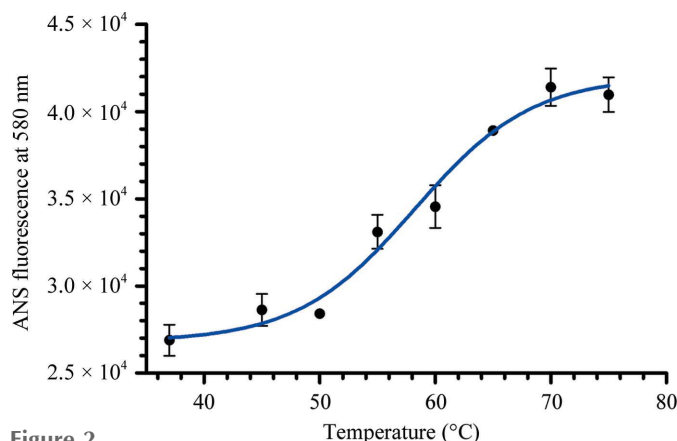


Figure 2
Thermal stability determination of AaL using ANS as a fluorescent probe.

solution. Diffraction-quality crystals appeared after 1 d at 292 K (Fig. 3).

2.5. Data collection

Crystals were transferred into a cryoprotectant solution consisting of the mother liquor supplemented with 20% (v/v) (final concentration) glycerol. The crystals were incubated for 1 min in the cryoprotectant solution and were subsequently mounted on a CryoLoop (Hampton Research) and flash-cooled at 100 K in liquid nitrogen. X-ray diffraction intensities were collected on the 23-ID-B beamline at the Advanced Photon Source (APS), Argonne National Laboratory, Lemont, Illinois, USA (Table 4). Diffraction experiments were

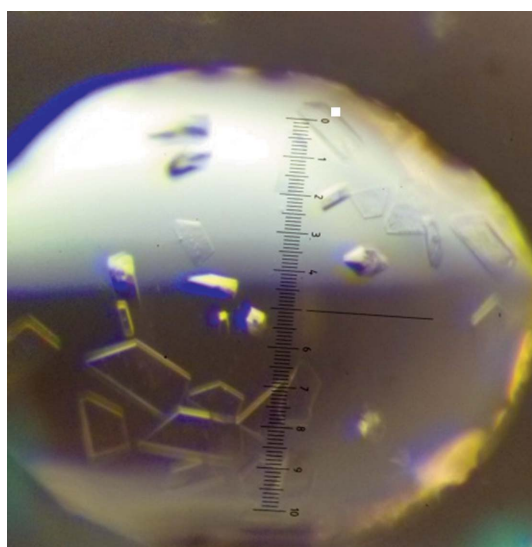


Figure 3
Typical crystals of the AaL protein. 1 scale unit = 110 μm .

Table 4

Data collection and processing.

Values in parentheses are for the outer shell.

Diffraction source	23-ID-B, APS
Wavelength (\AA)	1.033200
Temperature (K)	100
Detector	EIGER
Crystal-to-detector distance (mm)	200.0
Rotation range per image ($^\circ$)	0.2
Total rotation range ($^\circ$)	200
Exposure time per image (s)	0.2
Space group	C2
a, b, c (\AA)	111.72, 114.74, 79.97
α, β, γ ($^\circ$)	90.0, 109.8, 90.0
Resolution range (\AA)	1.65 (1.75–1.65)
Total No. of reflections	431338 (70385)
No. of unique reflections	111796 (17858)
Completeness (%)	98.2 (97.2)
Multiplicity	3.86 (3.94)
$\langle I/\sigma(I) \rangle$	22.08 (3.16)
$R_{\text{r.i.m.}}$ (%)	3.6 (59.1)

performed using a wavelength of 1.0332 \AA with 0.2 s exposures, and data were collected on an EIGER detector. Diffraction data were collected using the fine-slicing method; individual frames consisted of 0.2 $^\circ$ steps over a range of 1000 frames (Fig. 4).

3. Results and discussion

In this study, we provide the first characterization of a new lactonase, AaL, from the acidophilic, moderately thermophilic bacteria *A. acidoterrestris*. As expected, AaL is only a moderately thermostable enzyme (T_m of $58.2 \pm 1.1^\circ\text{C}$) and is less stable than the recently isolated lactonase GcL from *G. caldxylosilyticus* (half-life of 109.1 ± 7 min at 75°C ; Bergonzi *et al.*, 2016). Our kinetic data on various AHL substrates demonstrate that AaL is a proficient enzyme. It is

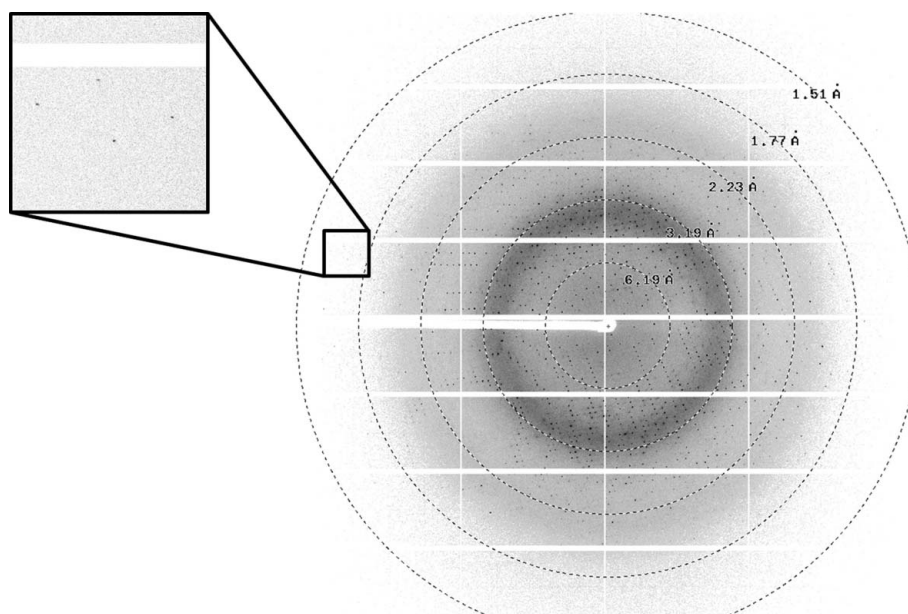


Figure 4
A diffraction frame from a crystal of AaL. The edge of the frame is at 1.23 \AA resolution.

among the most active lactonases characterized thus far, and is approximately tenfold more active than the well characterized AiiA against C6-HSL at 25°C (Momb *et al.*, 2008). In fact, AaL compares with GcL and is two orders of magnitude more active against C4-AHL (Bergonzi *et al.*, 2016). Kinetic measurements reveal that AaL exhibits similar hydrolysis rates independent of the AHL acyl-chain length, contrary to GcL (Bergonzi *et al.*, 2016) and PLLs, which show a marked preference for long-chain AHLs (Hiblot, Gotthard, Elias *et al.*, 2013). Solution of the structure of AaL is expected to shed light on the key structural determinants that account for its very unique broad substrate preference.

The lactonase AaL was therefore crystallized and diffraction data were collected to 1.65 Å resolution. The data were indexed, integrated and scaled using the *XDS* software package (Kabsch, 1993). The crystals belonged to space group C2, with unit-cell parameters $a = 111.72$, $b = 114.74$, $c = 79.97$ Å, $\alpha = \gamma = 90.0$, $\beta = 109.8^\circ$. With the molecular weight of AaL being 32.5 kDa, calculation of the Matthews coefficient suggested the presence of three monomers in the asymmetric unit (V_M of $2.47 \text{ \AA}^3 \text{ Da}^{-1}$ and 50.31% solvent content) as the most likely solution. Molecular replacement was performed using *MOLREP* (Vagin & Teplyakov, 2010) with the structure of AiiB as a starting model (PDB entry 2r2d; Liu *et al.*, 2007). After the initial molecular replacement, three molecules were placed in the asymmetric unit ($R = 34.30\%$, $R_{\text{free}} = 37.24\%$). Cycles of manual building and structure refinement using *REFMAC* (Murshudov *et al.*, 2011) allowed the model to be improved ($R = 17.5\%$, $R_{\text{free}} = 20.67\%$). The structure is still being improved by manual building using *Coot* (Emsley & Cowtan, 2004). Inspection of the electron-density maps suggests that apart from minor rotamers and solvent molecules the model is almost final, containing three molecules of AaL. Interpretation of the structure is currently in progress and will be published elsewhere.

Acknowledgements

We are grateful to the Nano Crystallization Facility and the Kahlert Structural Biology Laboratory, and in particular to Carrie Wilmot and Ke Shi for assistance in setting up crystallization screens and to Ed Hoeffner for assistance in using the in-house X-ray diffraction setup.

Funding information

The following funding is acknowledged: MnDrive Initiative; CTSI-ODAT grant; BioTechnology Institute Biocatalysis Award; United States–Israel Binational Agricultural Research and Development Fund (award No. IS-4960-16FR).

References

Afriat, L., Roodveldt, C., Manco, G. & Tawfik, D. S. (2006). *Biochemistry*, **45**, 13677–13686.
 Augustine, N., Kumar, P. & Thomas, S. (2010). *Arch. Microbiol.* **192**, 1019–1022.

Bar-Rogovsky, H., Hugenmatter, A. & Tawfik, D. S. (2013). *J. Biol. Chem.* **288**, 23914–23927.
 Bassler, B. L. (1999). *Curr. Opin. Microbiol.* **2**, 582–587.
 Ben-David, M., Sussman, J. L., Maxwell, C. I., Szeler, K., Kamerlin, S. C. & Tawfik, D. S. (2015). *J. Mol. Biol.* **427**, 1359–1374.
 Ben-David, M., Wiczorek, G., Elias, M., Silman, I., Sussman, J. L. & Tawfik, D. S. (2013). *J. Mol. Biol.* **425**, 1028–1038.
 Bergonzi, C., Schwab, M. & Elias, M. (2016). *Acta Cryst.* **F72**, 681–686.
 Bokhove, M., Nadal Jimenez, P., Quax, W. J. & Dijkstra, B. W. (2010). *Proc. Natl Acad. Sci. USA*, **107**, 686–691.
 Bzdrenga, J., Hiblot, J., Gotthard, G., Champion, C., Elias, M. & Chabriere, E. (2014). *BMC Res. Notes*, **7**, 333.
 Del Vecchio, P., Elias, M., Merone, L., Graziano, G., Dupuy, J., Mandrich, L., Carullo, P., Fournier, B., Rochu, D., Rossi, M., Masson, P., Chabriere, E. & Manco, G. (2009). *Extremophiles*, **13**, 461–470.
 Dong, Y.-H., Xu, J.-L., Li, X.-Z. & Zhang, L.-H. (2000). *Proc. Natl Acad. Sci. USA*, **97**, 3526–3531.
 Elias, M., Dupuy, J., Merone, L., Mandrich, L., Porzio, E., Moniot, S., Rochu, D., Lecomte, C., Rossi, M., Masson, P., Manco, G. & Chabriere, E. (2008). *J. Mol. Biol.* **379**, 1017–1028.
 Elias, M. & Tawfik, D. S. (2012). *J. Biol. Chem.* **287**, 11–20.
 Emsley, P. & Cowtan, K. (2004). *Acta Cryst.* **D60**, 2126–2132.
 Gotthard, G., Hiblot, J., Elias, M. & Chabriere, E. (2011). *Acta Cryst.* **F67**, 354–357.
 Hawe, A., Sutter, M. & Jiskoot, W. (2008). *Pharm. Res.* **25**, 1487–1499.
 Hawwa, R., Larsen, S. D., Ratia, K. & Mesecar, A. D. (2009). *J. Mol. Biol.* **393**, 36–57.
 Hiblot, J., Bzdrenga, J., Champion, C., Chabriere, E. & Elias, M. (2015). *Sci. Rep.* **5**, 8372.
 Hiblot, J., Gotthard, G., Chabriere, E. & Elias, M. (2012). *PLoS One*, **7**, e47028.
 Hiblot, J., Gotthard, G., Champion, C., Chabriere, E. & Elias, M. (2013). *Acta Cryst.* **F69**, 1235–1238.
 Hiblot, J., Gotthard, G., Elias, M. & Chabriere, E. (2013). *PLoS One*, **8**, e75272.
 Kabsch, W. (1993). *J. Appl. Cryst.* **26**, 795–800.
 Khersonsky, O. & Tawfik, D. S. (2005). *Biochemistry*, **44**, 6371–6382.
 Lade, H., Paul, D. & Kweon, J. H. (2014). *Biomed. Res. Int.* **2014**, 162584.
 LaSarre, B. & Federle, M. J. (2013). *Microbiol. Mol. Biol. Rev.* **77**, 73–111.
 Liu, D., Lepore, B. W., Petsko, G. A., Thomas, P. W., Stone, E. M., Fast, W. & Ringe, D. (2005). *Proc. Natl Acad. Sci. USA*, **102**, 11882–11887.
 Liu, D., Momb, J., Thomas, P. W., Moulin, A., Petsko, G. A., Fast, W. & Ringe, D. (2008). *Biochemistry*, **47**, 7706–7714.
 Liu, D., Thomas, P. W., Momb, J., Hoang, Q. Q., Petsko, G. A., Ringe, D. & Fast, W. (2007). *Biochemistry*, **46**, 11789–11799.
 Miller, M. B. & Bassler, B. L. (2001). *Annu. Rev. Microbiol.* **55**, 165–199.
 Momb, J., Wang, C., Liu, D., Thomas, P. W., Petsko, G. A., Guo, H., Ringe, D. & Fast, W. (2008). *Biochemistry*, **47**, 7715–7725.
 Murshudov, G. N., Skubák, P., Lebedev, A. A., Pannu, N. S., Steiner, R. A., Nicholls, R. A., Winn, M. D., Long, F. & Vagin, A. A. (2011). *Acta Cryst.* **D67**, 355–367.
 Schaefer, A. L., Greenberg, E., Oliver, C. M., Oda, Y., Huang, J. J., Bittan-Banin, G., Peres, C. M., Schmidt, S., Juhaszova, K., Sufirin, J. R. & Harwood, C. S. (2008). *Nature (London)*, **454**, 595–599.
 Spinelli, A. C. N., Sant’Ana, A. S., Rodrigues-Junior, S. & Massaguer, P. R. (2009). *Appl. Environ. Microbiol.* **75**, 7409–7416.
 Vagin, A. & Teplyakov, A. (2010). *Acta Cryst.* **D66**, 22–25.
 Xiang, D. F., Kolb, P., Fedorov, A. A., Meier, M. M., Fedorov, L. V., Nguyen, T. T., Sterner, R., Almo, S. C., Shoichet, B. K. & Raushel, F. M. (2009). *Biochemistry*, **48**, 2237–2247.